2016 American Control Conference (ACC)
Boston Marriott Copley Place
July 6-8, 2016. Boston, MA, USA

A Predictive Control Algorithm for Layer-to-layer Ink-jet 3D Printing

Yijie Guo[1] and Sandipan Mishra[2]

Abstract— **Ink-jet 3D printing is an additive manufacturing process where-in parts are built by jetting material from nozzles layer by layer, with curing between successive layers of deposition. Typically, this additive process is operated in an open-loop manner, i.e., the number of layers and droplet patterns for each layer are determined in advance and are not modified based on measurements of current height profile during the printing process. As a result, the uncertainties in droplet sizes, heights and locations during printing can result in undesired part geometry, such as edge shrinking, unreliable dimensions and uneven surfaces. Naturally, incorporating feedback measurements into the control algorithm will improve performance if suitable models and cost functions are constructed. In this paper, we first propose a control-oriented layer to layer height evolution model for two-material Ink-jet 3D printing. Based on this model, a predictive control algorithm that uses measurements of the current height profile to generate control inputs for successive layers is designed. The effectiveness of the proposed algorithm is demonstrated by simulation studies.**

I. INTRODUCTION

Additive manufacturing (AM) refers to the general class of manufacturing processes that build up three-dimensional objects layer by layer. The additive nature of these processes enables the efficient manufacturing of complex geometry parts. A large number of AM processes have been developed, with varying build materials and methods for material deposition. In this paper, we focus on ink-jet 3D printing, which has been widely used in commercial printers for its simplicity and small droplet size (10 to 500μm) [1].

Ink-jet 3D printing is typically executed in open-loop manner, which means the number of layers and droplet patterns for each layer are determined before the printing process. Furthermore, the determined droplet patterns are not modified based on any process measurements (e.g., current height profile, droplet size, etc.). As a result, any uncertainty in the printing process will result in undesirable printed part geometry, for example, edge shrinking, unreliable dimensions and surface unevenness [2]. This problem is exacerbated because of the complicated interactions between neighboring droplets and uncertain droplet dimensions.

For open-loop printing droplet patterns and geometry control, several models of the printing process and pre-compensation algorithms have been proposed, such as those in [3], [4]. In [3], a statistical predictive modeling and compensation approach for cylindrical and prismatic parts was proposed. In [4], a model was proposed to predict the part shrinkage and an optimal compensation plan was derived based on the model prediction. However, these methods are fundamentally feedforward in nature and do not address uncertainties that arise during the printing process. Hence, closed-loop control algorithms are necessary to compensate for the variability of the process.

Based on this need, of late, feedback control algorithms have also been proposed for ink-jet 3D printing. For example, in [5], a feedback control law for regulating droplet shape (i..e droplet height and/or diameter) was proposed. This algorithm only targeted droplet-level control and did not account for error at the whole-part geometry level. In [6], a search based closed-loop algorithm was proposed; the shape of each droplet was modeled as a spherical cap (based on the model introduced in [7]) and droplets were deposited at locations where the difference between the measurement and desired height was relatively large. However, surface evenness and the droplet's influence on its neighbors was not addressed. In [8], [9], an empirical layer-to-layer model was proposed and a feedback control algorithm was proposed based on it. This empirical model was shown to capture the edge shrinking effect, however, the feedback control law based on such a model needed a brute force search algorithm for determining the optimal printing patterns, which is extremely time-consuming. Therefore, we investigate the design of a predictive closed-loop control algorithm for ink-jet 3D printing that can deliver good performance (in terms of both dimensional accuracy and surface evenness) in a computationally tractable way.

In this paper, we propose a layer-to-layer height evolution model with a compact matrix form based on the single-layer model presented by Hoelzle and Barton in [10]. Note that while this simplified model cannot capture the edge shrinking phenomenon, the influence of edge shrinking on the printed part can be avoided by printing support material (sacrificial material). Thus, the proposed model is adequate when the primary focus is on achieving accurate dimensions and surface evenness. Furthermore, the proposed model structure captures two material layer-to-layer height change evolution. Based on this model, an optimization-based two-material printing algorithm using feedback height measurements is developed. The paper is organized as follows. The general two-material printing problem is stated in Sec. II. Then, the compact matrix form height evolution model is introduced in Sec. III. The proposed feedback control algorithm derived from optimization of a model-based cost function is then presented in Sec. IV, and the simulation results are demonstrated in Sec. V.

[1]Yijie Guo is with the Mechanical, Aerospace and Nuclear Engineering Department, Rensselaer Polytechnic Institute, Troy, NY 12180 USA guoy7@rpi.edu

[2]Sandipan Mishra is with faculty of the Mechanical, Aerospace and Nuclear Engineering Department, Rensselaer Polytechnic Institute, Troy, NY 12180 USA mishrs2@rpi.edu

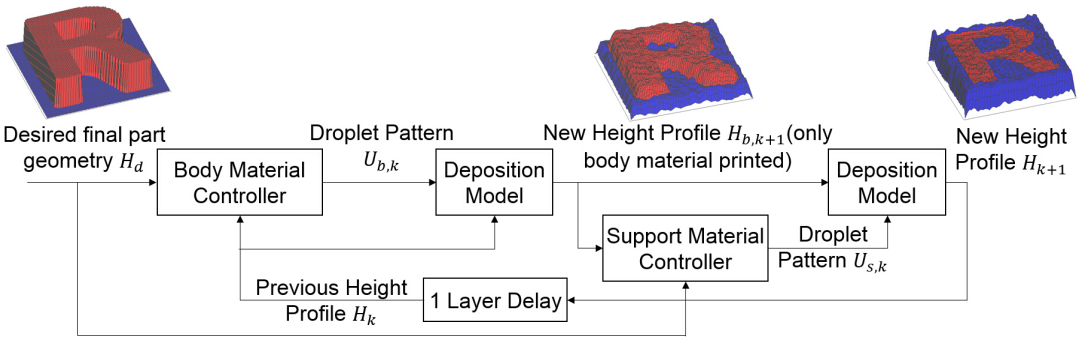

Fig. 1. A block diagram schematic of the closed-loop layer-to-layer printing process for two-material printing.

II. PROBLEM DESCRIPTION

In this section, we present the general formulation of the two-material printing problem for layer-to-layer ink-jet 3D printing. The block diagram of the printing process is shown in Fig. 1. For each layer, the printing is performed in two steps: first the body material is printed and then the support material is printed (for sharp edges and overhangs, etc.).

Based on this two step printing process, the surface can be separated into two parts M_b and M_s for each layer, which represent the (2D) regions where the body material and the support material are to be printed, respectively. The control input (droplet pattern/ sequence) to the system (i.e the plant) at the k^{th} layer is also separated into two parts $U_{b,k}$ and $U_{s,k}$. Two input forms are considered in this paper: in the first case, we only can decide whether or not to deposit a droplet at each location (called *Droplet Control*), and $U_{b,k}$, $U_{s,k} \in \{0,1\}^{n_x \times n_y}$ ($n_x \times n_y$ is the grid size of the printing region). The integers 1 and 0 denote whether or not the droplet is to be deposited. In the second case, the droplet volume at each location can be controlled (called *Volume Control*), thus $U_{b,k}$, $U_{s,k} \in [V_{min}, V_{max}]^{n_x \times n_y}$, where V_{min} and V_{max} are the minimum and maximum droplet volume we can control. Furthermore, in both cases, $U_{b,k}(i,j) = 0$ if $(i,j) \in M_s$, $U_{s,k}(i,j) = 0$ if $(i,j) \in M_b$. The desired part geometry is denoted by $H_d \in \{R^+\}^{n_x \times n_y}$. The height profile of the existing surface is denoted by $H_k \in \{R^+\}^{n_x \times n_y}$. First, the deposition process (height change model), uses the body material input $U_{b,k}$ and the prior height H_k to create $H_{b,k+1}$, the new layer height with only body material printed. Then the deposition process uses the support material input $U_{s,k}$ and $H_{b,k+1}$ to create the new layer H_{k+1}. Both $H_{b,k+1}$ and H_{k+1} are measured by the height/surface profile sensor. Mathematically, the height change is modeled by $H_{b,k+1} = f_m(H_k, U_{b,k})$, $H_{k+1} = f_m(H_{b,k+1}, U_{s,k})$. The body material controller uses the final desired part geometry and the measured current height to generate the appropriate droplet patterns for body material, the control law is given by $U_{b,k} = f_b(H_d, H_k)$, then the support material controller generates the droplet patterns for support material by $U_{s,k} = f_s(H_d, H_{b,k+1})$.

In the following two sections, we introduce a matrix form model that characterizes the layer-to-layer height evolution in Section III, then design a predictive optimization-based control algorithm based on this model in Section IV.

III. LAYER TO LAYER HEIGHT EVOLUTION MODEL

A. Layer to Layer Model

The height change process of the ink-jet 3D printing is naturally complicated to capture from a purely physics-driven modeling approach, based on the complex interactions between adjacent droplets (coalescence) and the initial surface's influence on the height change (surface energy interactions, etc.). In [7], Doumanidis et al. proposed that liquid droplet shape can be mathematically approximated using a lens model as in Fig. 2, and the height change was considered as the summation of droplet shape at each location. Lu et al. [8], [9] proposed an empirical model by identifying the height change caused by one droplet on its neighbors, which addressed both the influence of droplets interaction and initial surface. Hoelzle and Barton [10] proposed a matrix representation of a *2D printing process* also based on the idea that the height change is the summation of droplet shape at each location, which is simple and attractive from a control perspective. We adopt the matrix representation of height evolution model based on the lens model of single droplet. This matrix representation is developed below.

First, the print region and the droplet shape are discretized with grid size $n_x \times n_y$ and $d_x \times d_y$. Fig. 2 shows the discretized droplet shape. Then the droplet pattern U_k and height profile H_k can be rewritten into vector forms [10] $\mathbf{u}_k$ and $\mathbf{h}_k$, for example

$$U_k(x,y) = \begin{bmatrix} U_{1,1} & U_{1,2} & \cdots & U_{1,n_y} \\ U_{2,1} & U_{2,2} & \cdots & U_{2,n_y} \\ \vdots & \vdots & \ddots & \vdots \\ U_{n_x,1} & U_{n_x,2} & \cdots & U_{n_x,n_y} \end{bmatrix} \xrightarrow{\text{vectorize}} \begin{bmatrix} U_{1,1} \\ U_{1,2} \\ \vdots \\ U_{1,n_y} \\ U_{2,1} \\ \vdots \end{bmatrix} = \mathbf{u}_k. \tag{1}$$

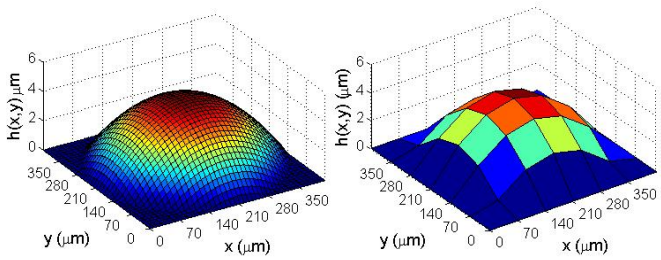

Fig. 2. Liquid droplet shape approximated using a lens model and the discretized droplet shape model. The grid size is $d_x = d_y = 7$.

Then the height evolution model can be captured by

$$\mathbf{h}_{k+1} = \mathbf{h}_k + G\mathbf{u}_k, \tag{2}$$

where $G \in \mathcal{R}^{N\times N}(N = n_x n_y)$ is obtained from lifted representation of 2D convolution, the details are in [10].

The height evolution models for body material printing and support material printing are

$$\mathbf{h}_{b,k+1} = \mathbf{h}_k + G\mathbf{u}_{b,k}, \tag{3}$$

$$\mathbf{h}_{k+1} = \mathbf{h}_{b,k+1} + G\mathbf{u}_{s,k}, \tag{4}$$

where $\mathbf{h}_{b,k+1} \in R^N$ is the height profile vector for $k+1$ th layer with only body material printed.

B. Model Uncertainty

During the printing process, the droplet volume varies based on operating environmental conditions, thereby introducing uncertainty to the droplet model. The height change of printing one layer can therefore be different from our identified open-loop layer height. We capture this modeling mismatch by adding uncertainty to the droplet control input,

$$\mathbf{u}_{\text{actual}} = \mathbf{u} \circ \mathcal{N}(1+\delta_1, \delta_2), \tag{5}$$

where $\mathcal{N}(1+\delta_1, \delta_2)$ is a vector of normally distributed numbers with a mean of $1+\delta_1$ and standard deviation δ_2, its length is the same as $\mathbf{u}$. The layer height uncertainty is captured by δ_1, if $\delta_1 > 0$, the actual layer height will be larger than the identified layer height, for example. The droplet volume uncertainty is captured by δ_2. In our simulation, we choose $\delta_1 = 0.1$, $\delta_2 = 0.25$.

In addition, the droplet shape can also vary based on operating environmental conditions. This can be captured by adding uncertainty to the matrix G.

$$G_{\text{actual}}(i,j) = G(i,j) \cdot \mathcal{R}(1, \delta_3), \tag{6}$$

where $\mathcal{R}(1, \delta_3)$ is a random number satisfying a normal distribution with a mean of 1 and standard deviation δ_3.

IV. CONTROL ALGORITHM

Based on the height evolution model introduced above, a predictive control law for the ink-jet printing process is proposed in this section. The layer separation and grid strategy, body material control and support material control algorithms are presented below.

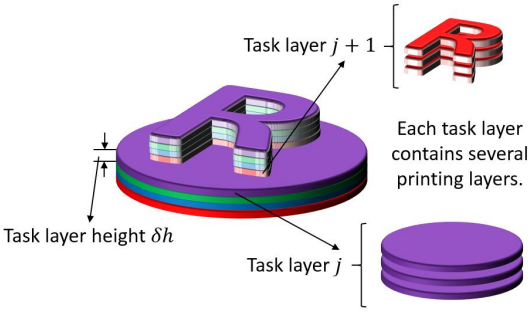

Fig. 3. Schematic of task layer separation. Several layers are printed for the realization of each task layer. The material region separation is assumed to be identical in each task layer, which is reasonable if δh is small enough.

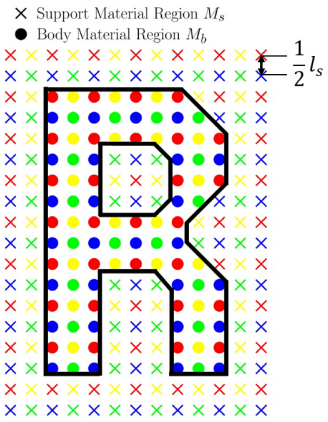

Fig. 4. A schematic sketch of the gridding of the printing region, where the block 'R' is the desired geometry for this particular task layer. The grid size is half of the line spacing used. Circles indicate the body material region, while crosses indicate the support material region. The colors (red, blue, green, and yellow) indicate the droplets that are deposited in the same layer, i.e., at each layer staggered droplet locations are deposited.

A. Layer Separation and Grid Strategy

1) Layer Separation: Given a desired final part geometry, we first separate the geometry into several *task layers* with a height of δh (typically two-five times the average open-loop layer height). The schematic of layer separation is shown in Fig. 3. Note that the task layers here do not refer to the printing layers. Instead, several layers will be printed for the realization of each single task layer. Now, each task layer is separated into two regions M_b and M_s in the printing plane (x, y) based on the material type to be deposited. We assume that the material region separation is identical in each task layer, which is reasonable if δh is small.

After the task layer separation, at the j^{th} task layer, the desired height $hd^{(j)}$ and material separation region $M_b^{(j)}$ and $M_s^{(j)}$ is known and fixed. Bases on this knowledge, we will use the optimization based control algorithm presented later to realize this task layer accurately. After one task layer is completed, $hd^{(j+1)}$ is set to $hd^{(j+1)} = hd^{(j)} + \delta h$. Then based on $hd^{(j+1)}$, $M_b^{(j+1)}$ and $M_s^{(j+1)}$, we again use the proposed control algorithm to realize the $j+1^{th}$ task layer.

2) Choosing Grid Size: The grid size of the printing region and droplet shape is usually determined according to the line spacing (distance between droplets) used in ink-jet printing. Practically, for a certain material, the line spacing is usually determined so that: (1) when all the points are printed onto a layer, the top layer(surface) is the smoothest and (2) neighboring droplets does not overlap too much to prevent strong coalescing and flow effects [9].

When the line spacing is determined (l_s), the grid size is set as $\frac{l_s}{2}$, as shown in Fig. 4. We only print on one fourth of the grid points for each layer. For example, we will decide the droplet pattern only on the red circles or crosses in the first layer, then in the second layer, the droplet pattern will only be decided on the yellow circles or crosses, then green and blue, the printing will be repeated in this order in the following layers.

The control algorithms for body material printing and support material printing to realize each task layer are presented below.

B. Body Material Control Algorithm

The body material control algorithm (for a task layer) is presented in this section. To realize the j^{th} task layer, several layers must be printed. The final desired height is $h_d^{(j)}$ for the j^{th} task layer. In this section, we will drop the superscript j and use h_d for simplicity of notation. After one task layer is completed, h_d is set to the next desired task layer height $h_d^{(j+1)}$ as described in Sec. IV-A.

To ensure that the final printed part geometry is as close to the desired part geometry as possible, we want to track each *task layer* accurately in terms of both the height and the surface evenness. In the body material printing step, we only control $\mathbf{u}_{b,k}$, the droplet input in body material region, and only care about the height profile and surface evenness over the body material region.

1) Volume Control Case: For the volume control case, we assume that we can control the droplet volume. The droplet shape is modeled as a droplet with maximum volume, thus $V_{max} = 1$, and the minimum volume is $V_{min} = 0$, which means no droplet is deposited. The control goal can be captured by an optimization problem

$$\begin{array}{ll} \min\limits_{\mathbf{u}_{b,k}} & \|Q(\mathbf{h}_d - \mathbf{h}_{b,k+1})\|_2^2 + \alpha \cdot Var(Q\mathbf{h}_{b,k+1}) \\ \text{subject to} & 0 \le \mathbf{u}_{b,k}(\cdot) \le 1,\ \mathbf{u}_{b,k}(i) = 0 \text{ if } i \in M_s \end{array}, \tag{7}$$

where $\mathbf{h}_d = h_d \mathbf{1}_N$, $\mathbf{1}_N$ is the vector of 1s with length N. The matrix $Q \in \mathcal{R}^{N_b \times N}$ transfers the height profile from whole region to body material region (Number of points $= N_b$). The variance of the body material region $Var(Q\mathbf{h}_{b,k+1})$ can be defined as $\|D_{N_b} Q\mathbf{h}_{b,k+1}\|_2^2$, where

$$D_{N_b} = \begin{bmatrix} 1 & -\frac{1}{N_b-1} & \cdots & -\frac{1}{N_b-1} \\ -\frac{1}{N_b-1} & 1 & \cdots & -\frac{1}{N_b-1} \\ \vdots & \vdots & \ddots & \vdots \\ -\frac{1}{N_b-1} & -\frac{1}{N_b-1} & \cdots & 1 \end{bmatrix}. \tag{8}$$

The coefficient α is the trade off between height tracking and surface evenness.

This optimization problem is a QP (Quadratic Programming) problem

$$\begin{array}{ll} \min\limits_{\mathbf{u}_{b,k}} & \|Q(\mathbf{h}_d - \mathbf{h}_k - G\mathbf{u}_{b,k})\|_2^2 + \alpha \|D_{N_b} Q(\mathbf{h}_k + G\mathbf{u}_{b,k})\|_2^2 \\ \text{subject to} & 0 \le \mathbf{u}_{b,k}(\cdot) \le 1,\ \mathbf{u}_{b,k}(i) = 0 \text{ if } i \in M_s \end{array}, \tag{9}$$

Thus $\mathbf{u}_{b,k}$ can be calculated by solving this optimization problem. Note that the *feedback measurement* of the height profile $\mathbf{h}_k$ is necessary to solve this optimization problem.

2) Droplet Control Case: For the droplet control case, we can only control whether or not a droplet can be deposited. Thus, the control problem can be captured by the following MIQP (Mixed Integer Quadratic Programming) problem

$$\begin{array}{ll} \min\limits_{\mathbf{u}_{b,k}} & \|Q(\mathbf{h}_d - \mathbf{h}_k - G\mathbf{u}_{b,k})\|_2^2 + \alpha \|D_{N_b} Q(\mathbf{h}_k + G\mathbf{u}_{b,k})\|_2^2 \\ \text{subject to} & \mathbf{u}_{b,k}(\cdot) \in \{0,1\},\ \mathbf{u}_{b,k}(i) = 0 \text{ if } i \in M_s \end{array}. \tag{10}$$

However, MIQPs are often nonconvex (as in this case) and therefore difficult and time-consuming to solve. Therefore, to avoid these long calculation times, we propose a sub-optimal two-step fast implementation of the MIQP based algorithm.

First, instead of solving the MIQP problem in (10), we will solve the same constrained QP problem as (9), and get the solution $\bar{\mathbf{u}}_{b,k}$. Such constrained QPs can be efficiently solved using existing solver packages such as CPLEX [11].

Then the second step is to then project the continuous solution to binary solution. The solution of (9) can be considered as a threshold to release a droplet at a location. Thus, to get $\mathbf{u}_{b,k}$ from $\bar{\mathbf{u}}_{b,k}$, we can use

$$\mathbf{u}_{b,k}(\cdot) = \begin{cases} 1, \text{ if } \bar{\mathbf{u}}_{b,k}(\cdot) \ge 0.5 \\ 0, \text{ if } \bar{\mathbf{u}}_{b,k}(\cdot) < 0.5 \end{cases}. \tag{11}$$

C. Support Material Control Algorithm

After the body material has been printed, the support material is printed to make the surface flat and fill the voids. Note that in this step, we care about the surface evenness of the entire region.

1) Volume Control Case: For the volume control case, the control goal can be captured by the following optimization problem.

$$\begin{array}{ll} \min\limits_{\mathbf{u}_{s,k}} & Var(\mathbf{h}_{k+1}) \\ \text{subject to} & 0 \le \mathbf{u}_{s,k}(\cdot) \le 1 \\ & \mathbf{u}_{s,k}(i) = 0 \text{ if } i \in M_b \end{array}. \tag{12}$$

Similarly this optimization can also be written as a QP problem

$$\begin{array}{ll} \min\limits_{\mathbf{u}_{s,k}} & \|D_N(\mathbf{h}_{b,k+1} + G\mathbf{u}_{s,k})\|_2^2 \\ \text{subject to} & 0 \le \mathbf{u}_{s,k}(\cdot) \le 1 \\ & \mathbf{u}_{s,k}(i) = 0 \text{ if } i \in M_b \end{array}. \tag{13}$$

Thus $\mathbf{u}_{s,k}$ can be calculated by solving this optimization problem after body material has been deposited. Note that the *feedback measurement* of the height profile $\mathbf{h}_{b,k+1}$ is

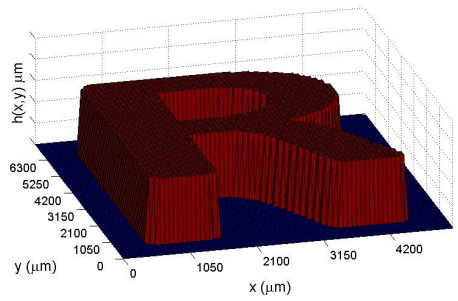

Fig. 5. The desired part geometry. For volume control case, the height is 180 μm, for droplet control case, the height is 306 μm.

necessary to solve this optimization problem.

2) Droplet Control Case: For the droplet control case, the control goal can be captured by an MIQP problem

$$\begin{array}{ll} \min\limits_{\mathbf{u}_{s,k}} & \|D_N(\mathbf{h}_{b,k+1} + G\mathbf{u}_{s,k})\|_2^2 \\ \text{subject to} & \mathbf{u}_{s,k}(\cdot) \in \{0,1\} \\ & \mathbf{u}_{s,k}(i) = 0 \text{ if } i \in M_b \end{array} . \quad (14)$$

We then follow the same process as in the body material control section to obtain the binary solution, i.e., first we solve the constrained QP problem (13) and then use the same process as in (11) to obtain $\mathbf{u}_{s,k}$.

The optimization based control algorithm proposed above is based on a 2-norm type cost function. The cost function can also include ∞-norm of error and the constructed optimization problems can be reformulated as LP and MILP problems, similar to [12]. Details are omitted in this paper.

V. SIMULATION RESULTS

We have presented an optimization based control algorithm. In this section, the simulation results of the proposed printing control algorithm and the comparison with open-loop printing will be illustrated.

A. Volume Control Case

We choose the solid character 'R' as the desired geometry, as shown in Fig. 5. The desired height is chosen as 180 μm ($180 = 20 \times 9$), based on the fact that open-loop printing one layer height is 9 μm (obtained from optimization based on the droplet model shown in Fig. 2). The task layer height is chosen as $\delta h = 18$ μm, twice the open-loop layer height.

We now compare the simulated printed parts using the proposed control algorithm and open-loop printing (for printing 20 layers). The two printed parts are shown in Fig. 6. The top surface data are shown in Tab. I. We can observe that the printed part using the proposed algorithm has better surface evenness. Furthermore, the average height of the printed parts using the proposed algorithm is 182 μm, which is close to the desired height 180 μm, while the average height of the printed part using open-loop printing is 198 μm. Thus, the proposed feedback control algorithm can achieve better performance than the traditional open-loop printing in the volume control case, in terms of both height tracking and surface evenness.

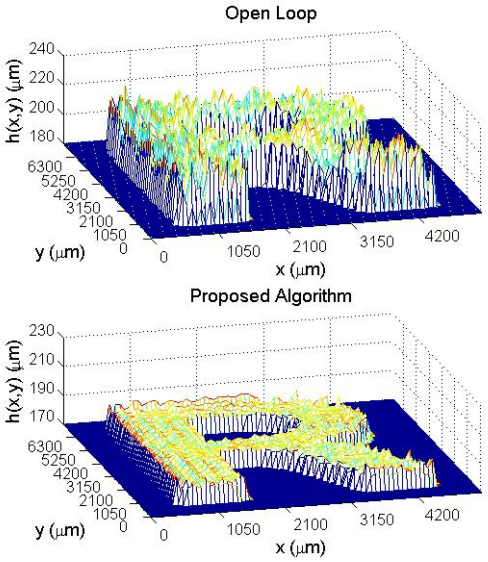

Fig. 6. The top surface of printed parts in the volume control case. The printed part using the proposed algorithm has better surface evenness and height accuracy.

TABLE I
SUMMARY OF VOLUME CONTROL CASE SIMULATION RESULTS

Top Surface	Desired Part	Open-loop Printing	Proposed Algorithm
Mean	180 μm	198 μm	182 μm
SD	0 μm	13 μm	2 μm

B. Droplet Control Case

As in the previous case, we choose the character 'R' as our desired geometry, which is shown in Fig. 5. The desired height is chosen as 306 μm ($306 = 20 \times 15.3$), this is based on the fact that open-loop printing one layer height is 15.3 μm (obtained from optimization). In our proposed closed-loop control algorithm, the task layer height is chosen as $\delta h = 30.6$ μm, twice the open-loop layer height.

We now compare the simulated printed parts using the proposed control algorithm and open-loop printing (print 20 layers). The two printed parts are shown in Fig. 7. The top surface data are shown in Tab. II. We can observe that the printed part using the proposed algorithm has better surface evenness and height accuracy, its average height is 308 μm, which is close to the desired height 306 μm, while the average height of the printed part using open-loop printing is 336 μm. Thus, the proposed control algorithm can achieve better performance than the traditional open-loop printing in the droplet control case, in terms of both height tracking and surface evenness.

C. Application to Non-extruded Part Geometry

Simulation results for an extruded part were shown above, where the material deposition regions are the the same for all the task layers. A simple case with two different material

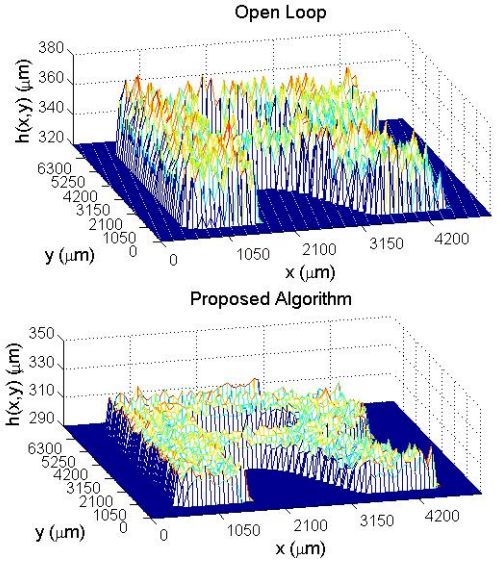

Fig. 7. The top surface of printed parts in the droplet control case. The printed part using the proposed algorithm has better surface evenness and height accuracy.

TABLE II
SUMMARY OF DROPLET CONTROL CASE SIMULATION RESULTS

Top Surface	Desired Part	Open-loop Printing	Proposed Algorithm
Mean	306 μm	336 μm	308 μm
SD	0 μm	22 μm	4 μm

separation regions is shown in Fig. 8 to demonstrate the ability of the proposed algorithm to print a non-extruded part. Note that, a complicated geometry can also be separated into the task layers with different material separation regions, and thus can be printed using the proposed algorithm.

D. Computation Times

A rough order of magnitude estimate of the time of the proposed algorithm is presented here. The simulation was run on a desktop using MATLAB with Intel(R) Core(TM) i7-4790 CPU @ 3.60GHz 3.60GHz and 16GB RAM. MATLAB solver 'quadprog' with default algorithm 'interior-point-convex' was used in the proposed algorithm. For the character 'R' case, the grid size was 100×70, the proposed algorithm required 3 to 5 seconds to calculate one printing layer.

VI. CONCLUSION

In this paper, an optimization based two-material printing control algorithm based on a control oriented layer-to-layer height evolution model was proposed to address the issue of undesired part brought by printing process uncertainty. The effectiveness of this control algorithm was verified though simulations. We observed that the proposed algorithm has better performance in terms of both height tracking and surface evenness than open-loop printing. With this control

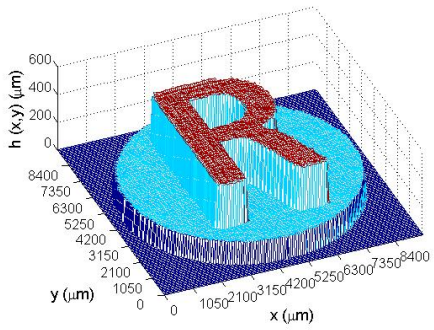

Fig. 8. The geometry of character 'R' on a circle base printed using our proposed algorithm in the droplet control case.

algorithm, future work will include experimental validation and (numerically) efficient optimization algorithms.

ACKNOWLEDGMENT

This work was supported in part by the National Science Foundation Career Award grant CMMI-1254313 and in part by the Center for Automation Technologies and Systems (CATS) under a block grant from the New York State Empire State Development Division of Science, Technology and Innovation (NYSTAR).

REFERENCES

[1] P. Cooley, D. Wallace, and B. Antohe, "Applicatons of ink-jet printing technology to biomems and microfluidic systems," *Journal of the Association for Laboratory Automation*, vol. 7, no. 5, pp. 33–39, 2002.

[2] B. Derby, "Inkjet printing ceramics: From drops to solid," *Journal of the European Ceramic Society*, vol. 31, no. 14, pp. 2543–2550, 2011.

[3] Q. Huang, H. Nouri, K. Xu, Y. Chen, S. Sosina, and T. Dasgupta, "Statistical predictive modeling and compensation of geometric deviations of three-dimensional printed products," *Journal of Manufacturing Science and Engineering*, vol. 136, no. 6, p. 061008, 2014.

[4] Q. Huang, J. Zhang, A. Sabbaghi, and T. Dasgupta, "Optimal offline compensation of shape shrinkage for three-dimensional printing processes," *IIE Transactions*, vol. 47, no. 5, pp. 431–441, 2015.

[5] J. Mazumder, A. Schifferer, and J. Choi, "Direct materials deposition: designed macro and microstructure," *Material Research Innovations*, vol. 3, no. 3, pp. 118–131, 1999.

[6] D. L. Cohen and H. Lipson, "Geometric feedback control of discrete-deposition sff systems," *Rapid Prototyping Journal*, vol. 16, no. 5, pp. 377–393, 2010.

[7] C. Doumanidis and E. Skordeli, "Distributed-parameter modeling for geometry control of manufacturing processes with material deposition," *Journal of dynamic systems, measurement, and control*, vol. 122, no. 1, pp. 71–77, 2000.

[8] L. Lu, J. Zheng, and S. Mishra, "A model-based layer-to-layer control algorithm for ink-jet 3d printing," in *Dynamic Systems and Control Conference (DSCC), 2014*. ASME, 2014, p. V002T35A001.

[9] ——, "A layer-to-layer model and feedback control of ink-jet 3-d printing," *Mechatronics, IEEE/ASME Transactions on*, vol. 20, no. 3, pp. 1056–1068, 2015.

[10] D. J. Hoelzle and K. L. Barton, "A new spatial iterative learning control approach for improved micro-additive manufacturing," in *American Control Conference (ACC), 2014*. IEEE, 2014, pp. 1805–1810.

[11] "Ibm ilog cplex optimizer," [Accessed 27-September-2015]. [Online]. Available: http://www-01.ibm.com/software/commerce/optimization/cplex-optimizer/

[12] Y. Guo and S. Mishra, "Constrained optimal iterative learning control for mixed-norm cost functions," in *American Control Conference (ACC), 2015*. IEEE, 2015, pp. 4886–4891.